

Controller Design for Flexible, Distributed Parameter Mechanical Arms Via Combined State Space and Frequency Domain Techniques

W. J. Book

M. Majette¹

School of Mechanical Engineering,
Georgia Institute of Technology,
Atlanta, Ga 30332

The potential benefits of the ability to control more flexible mechanical arms are discussed. A justification is made in terms of speed of movement. A new controller design procedure is then developed to provide this capability. It uses both a frequency domain representation and a state variable representation of the arm model. The frequency domain model is used to update the modal state variable model to insure decoupled states. The technique is applied to a simple example with encouraging results.

1 Introduction

The justification for controlling compliant arms and other mechanical devices need be none other than the justification for controlling the device in the first place. All mechanical devices are subject to deformation under loading and hence are compliant. It is appropriate to ask if one is willing to concede lower performance in order to justify the assumption of a rigid mechanical linkage. When performance demands are not severe one can afford this luxury, compensating for the extra mass of the moving parts with larger actuators. Even in these cases one should look at the cost effectiveness of the "easy" solution. The control of compliant or flexible arms is not of interest only in space applications or as an exercise in control theory but can impact probably every arm design that strives for higher performance.

The desire to avoid the control of compliant arms is understandable from a practical point of view. The complex nonlinear dynamics of a six degree of freedom arm give the designer enough problems without adding to them the untried techniques of compliant arm control. This makes the problem a suitable research topic. The advantages to be gained from a compliant arm control capability are several and diverse. They include:

- higher speed
- smaller actuators
- lower energy consumption
- lower overall cost
- safer operation due to reduced inertia
- less bulky design
- enhanced back-driveability due to elimination of gearing

- lower overall mass to be transported (useful for both space and earthly applications)
- lowered mounting strength and rigidity requirements

It is obvious on examining the above list that the items are not independent. Actuator size cannot be reduced and the full increase in speed be realized, for example.

It is difficult to "prove" or even demonstrate in a general way the potential advantages resulting from a compliant arm capability in any of the above categories. The first part of this paper will attempt to demonstrate the advantages in terms of speed of motion for a simple arm-like configuration. The assumptions are reasonable ones but are fairly simple and could be disputed. The purpose is not to attempt a proof but to indicate the potential and for what type of arm that potential would be greatest.

The second part of the paper discusses the compliant arm modeling problem. Two methods considered are the frequency domain model implemented with the transfer matrix approach and the state variable time domain model with a model representation of the distributed arm elements. The two approaches are discussed briefly with the advantages of each and how they can complement each other in a control design algorithm.

The third part of the paper discusses one control design technique utilizing both models discussed above. Control gains for placement of the poles of the lower order state variable model are found. The control is then incorporated in the frequency domain analysis which is used to update the state variable model. The algorithm converges to the proper control gains to place the poles of the infinite dimensional distributed parameter system at the desired locations in the examples attempted. No proof of that convergence has been attempted. Several examples are presented.

¹Currently, Hewlett-Packard Inc., San Diego, Calif. 92127

Contributed by the Dynamic Systems and Control Division for publication in the JOURNAL OF DYNAMIC SYSTEMS, MEASUREMENT, AND CONTROL. Manuscript received by the Dynamic Systems and Control Division, June 28, 1982.

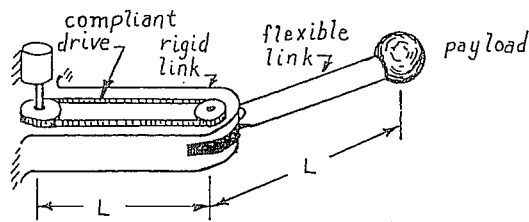


Fig. 2-1 Example arm for evaluation of compliant arm control potential

2 The Potential Payoff in Compliant Arm Control

As mentioned in the introduction there are many ways a compliant arm control capability could improve mechanical arm design. In this section one of these ways, decreased movement time, is explored in a fairly general way. This section is included to provide incentive to the more practically minded reader. More detailed consideration and more realistic assumptions than those employed here can of course be made, but at the expense of complicating the analysis beyond comprehension. The intent is not to "prove" in any rigorous sense that compliant arm control will pay off in given circumstances, but to make plausible that pay off. The final proof awaits the complete design of a practical compliant arm.

2.1. A Simple Example Arm. As a vehicle for exploring the potential payoff of compliant arm control a simple stereotypical arm is proposed in Fig. 2-1. It consists of a rigid first link of length L and a flexible second link of length L . They are connected by a rotary joint driven through a flexible drive by an actuator at the base of the first link. In Fig. 2-1 the drive is depicted as a belt but any member loaded primarily in tension and compression would be equivalent for the purposes of this analysis except that the radius of the pulley is chosen to be the same as the radius of the second link. This mechanical advantage could be representative of other drive arrangements as well.

The simple example arm has compliant members of both the distributed type (the link) and the lumped type (the drive is assumed to behave as a simple spring). The rigid first link reflects the lower penalty one pays for this added mass since the actuator which would move it could itself be stationary. The assumption of a rigid first link results in a conservative prediction of the worth of a compliant arm control. A point mass representing the end effector and the payload are located on the end of the second link.

In order to generate a large number of designs as the arm design parameters are varied the design must be done automatically. This requires the institution of certain design rules relating parameters in a reasonable way. The alternative of optimizing all design parameters is unattractive because a) realistic performance criteria are not known, and b) the computation cost would be prohibitive. The sizing of the drive pulley is an example of a design rule already mentioned. The design rules are listed below:

1. The link cross sections are concentric circles, with inner radius $.9 \times$ outer radius. The cross sections are constant over the length.
2. Material can be added to either the drive or the link in order to increase rigidity. The distribution is made so that total inertia experienced by all motors is minimized.
3. The pulley radius is equal to the outer radius of the second link.

2.2 Constraints in Sizing Structural Members. The sizing of structural members of a mechanical arm, including the links, is constrained in a number of ways. A partial list would include

1. Strength (Maximum stress)
2. Rigidity
3. Buckling in various modes
4. The allowable envelope of the work space
5. Internal envelope of components housed inside the member.

Only the first two constraints will be considered here in any detail.

2.2.1 The Strength Constraint. The most commonly used criteria for evaluating the adequacy of a structural member is the maximum stress that it will experience. In the case of our simple example arm only two design parameters are available to increase the strength: the radius and the material. Further specifying the material then requires that for adequate strength

$$R > R_{\text{strength}}$$

Since it is anticipated that the links of the example arm will be slender the equation for bending stress in simple beams is appropriate:

$$\begin{aligned}\sigma_{\text{max}} &= Mc/I = MR/[\pi(R^4 - r^4)/4] \\ \sigma_{\text{max}} &= 3.7M/R^3\end{aligned}$$

where M is the moment at a given cross section. This moment is typically greatest at the point nearest the fixed end of the arm. It depends on the mass of the payload, the accelerations of the link, including gravity, and the mass of the link itself. The moment at the proximal end of the link can also be specified in terms of the joint torque provided by the actuator and drive. The accelerations can be specified in terms of the motion time which is possible for a given acceleration profile. The final form assumes all the design rules mentioned above. Knowing the moment and the maximum allowable stress for the material one can determine the minimum radius R allowable on the basis of strength.

2.2.2 The Stiffness Constraint. Stiffness or rigidity of a mechanical arm is important in a static sense to avoid excessive static deflection and in a dynamic sense. The dynamic effects of rigidity, or the lack of it, include dynamic positioning errors and more importantly the adverse effect on control system stability. This is the constraint which will be considered here.

The rigidity necessary to insure proper control system operation depends on the control algorithm. For simple linear position and velocity feedback control of joint torque it has been found [4] that for a similar configuration the constraint could be stated in terms of the natural frequency of the arm with the actuators clamped or rigidized. When an eigenvalue of the controlled arm exceeded in magnitude about .28 times the clamped actuator natural frequency it was found that this simple control algorithm could no longer achieve critical damping of the dominant mode. A damping ratio of 0.707 could not be achieved with eigenvalue magnitudes greater than 0.386 times the clamped actuator natural frequency. Hence a rule of thumb was given in that work that the clamped actuator natural frequency of the arm must exceed α times the desired servo bandwidth in order to achieve adequate damping of the dominant eigenvalues. For position and velocity feedback control α is approximately three.

The design parameters available in the example arm used here to achieve the required clamped actuator natural frequency include once again the material and the link radii. In addition the cross section of the joint drive and its material are important. This relationship is not simple or explicit if we model the distributed nature of the mass and compliance of the link. Furthermore, the sizing problem is underconstrained even if we specify the materials. One can find many com-

binations of link and drive cross section which will achieve a given natural frequency. In this study the distribution of material between the link and the drive was done in a way to minimize the total inertia that all actuators must move. Since the outer link must be driven by actuators of all joints in-board, a greater penalty is placed on that inertia.

The result of this approach is that the radius of the outer link, R must be greater than a certain minimum in order to provide the required rigidity.

$$R > R_{\text{stiffness}}$$

Consequently there exist two constraint radii, one, R_{strength} , dictated by strength (stress) and one, $R_{\text{stiffness}}$ dictated by rigidity. If $R_{\text{strength}} > R_{\text{stiffness}}$ then stiffness is not an issue in arm design. If $R_{\text{stiffness}} > R_{\text{strength}}$, then the latter indicates a limit beyond which further improvements in control system capability to handle flexible behavior do not improve the arm design.

2.3 The Speed Penalty in Sizing Structural Members. One way to demonstrate the penalty for requiring more rigid arms is in terms of the reduction in speed. If a control algorithm were available which eliminated the stiffness constraint the arm radius R would equal R_{strength} . Actuators could then be sized to achieve a given movement in a specified time. The same actuators used in a design where $R = R_{\text{stiffness}} (> R_{\text{strength}})$ would move the arm more slowly. This reduction in speed has been determined for a number of cases.

The Fig. 2-2 shows the results of such an exercise for a range of arm lengths and payload masses. The speed of the arm is indicated in terms of the angle the joint moves divided by the square of the time to move through that angle. The actuator is assumed to be a torque limited torque source with the maximum torque applied first in one direction to accelerate the arm, then in the other direction to decelerate the arm (bang-bang control). The motion is assumed to be perpendicular to any gravitational field. Angle over time squared is displayed because it depends only on the inertia and the actuator torque as shown below.

$$\theta/T^2 = M/4J$$

where

- θ = the angle moved
- T = the time required for moving to and stopping at the new position
- M = the actuator torque applied to the rotary joint the moment on the cross section
- J = the mass moment of inertia of the arm and payload about the joint axis

Figure 2-2 is typical of a wide range of assumed values for material parameters, maximum values of θ/T^2 , and required clamped joint frequencies. For example, an arm with $L = 1.4$ m carrying 10kg could be designed to move π radians in one second and stop without failing. If the cross section is increased to achieve adequate stiffness the angle moved by the same actuator drops to approximately 1.5 radians in one second. Several interesting observations can be made on the basis of these studies.

- The assumption that $R_{\text{strength}} < R_{\text{stiffness}}$ is justified.
- A substantial penalty is paid in terms of speed for stiffening the arm. In the example a reduction of the angle traveled of 50 percent is observed.
- The penalty is greatest for longer arms and lighter payloads. This is obvious from the order and shape of the curves.
- The penalty is greater for relatively high strength, low rigidity materials with high density. This was observed from comparing a number of curves of the form of 2-2.

Caution is necessary when interpreting the results in an

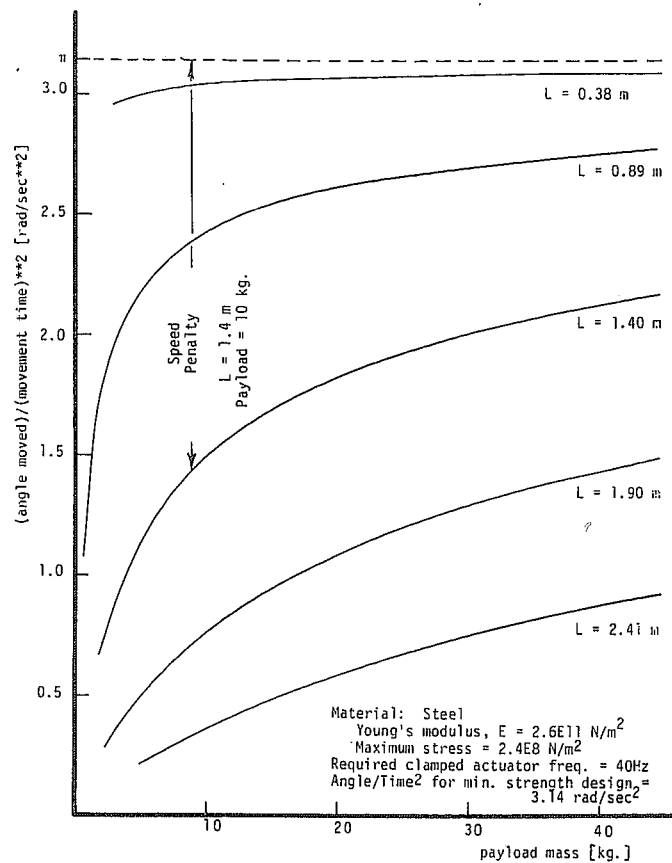


Fig. 2-2 Speed penalty for a steel arm

absolute sense. The reduction in the multiplier α that would be necessary to remove all the penalty from the loading arms is substantially greater for the long arms. The specifics of the analysis can be modified but the consistent result is that the penalty paid for rigidizing the arm to the extent necessary to use the simple position and velocity servo control of a rigid arm is substantial and warrants development of techniques to include arm compliance in the model.

3 Complaint Arm Models

In this section two complimentary models for flexible arm dynamics are discussed: the modal state variable model, and the frequency domain model implemented with transfer matrix techniques. After introduction of the modeling approaches, a way of transforming between the two models is presented, with emphasis on transforming from the frequency domain to the state variable model.

3.1. The State Variable Model With Modal Coordinates. The state variable model formulation has been extremely valuable in formulating control problems in a way which is amenable to computer aided design. The linear version in particular has been valuable. The formulation is given by the equation:

$$\begin{aligned} dx/dt &= Ax + Bu \\ y &= Cx + Du \end{aligned} \quad (1)$$

where

- x = the state vector, dimension $1 \times n$
- A = the plant matrix, dimension $n \times n$
- B = the control matrix, dimension $m \times n$
- u = the control vector, dimension $1 \times m$
- y = the output vector, dimension $1 \times p$
- C = the output matrix, dimension $p \times n$
- D = the feed through matrix, dimension $p \times m$

Linear transformations enable the description of the dynamics of the system to be described in many compatible forms with different state variables. Of particular interest is the Jordan canonical form in which the plant matrix $A = \Lambda$ contains explicitly the eigenvalues of the system. If eigenvalues are not repeated Λ is diagonal. The state variables in x in this case are called the modal coordinates.

An approximation to the dynamics of infinite dimensional systems is often made which incorporates the Jordan form of the state equations. This relies on the fact that the slower, lower frequencies alone are often adequate to describe the phenomena of interest. Since in the Jordan canonical form the low (frequency) modes are decoupled from the higher (frequency) modes, a clear understanding of the nature of the approximation is possible. The conditions under which this approximation is possible is discussed by Murray-Lasso [9]. When an infinite dimensional system with a true modal description is modified by incorporating a control vector u the equations are no longer, in general, decoupled. The parasitic effect of the excluded degrees of freedom (residual modes) is called "spillover" by Balas [1] and others. The effect of this distortion is often ignored. Indeed many models of infinite dimensional systems combine components described by their modes (component modes). These modes are obtained from idealized boundary conditions not present in the complete, composite model, resulting in the initial "modal" model not being decoupled and hence not being a truly modal model. The justification for this is similar to that used in a lumped parameter or discretized model of the system. The lower modes of the model are assumed to be accurate while the higher modes of the model are inaccurate and ignored. They must be included, however, to promote the accuracy of the low modes. The efficiency of the model in terms of the total number of modes that must be included to assure the needed accuracy is usually improved by using component modes for system coordinates. The number of component modes needed and the resulting accuracy of the system modes is always in question.

3.2 The Frequency Domain Model Using Transfer Matrices. When the dynamics of an infinite dimensional system can be represented by a linear partial differential equation of order N , classical frequency domain techniques can be applied with good success. Separation of variables is assumed whereby the response w can be written as

$$w(z,t) = w_z(z)w_t(t)$$

where

- w = the response of the system at a point in space and time
- z = the independent spatial variable
- t = the independent time variable
- w_z = a function of only space
- w_t = a function of only time

When this assumed form is substituted into the partial differential equation, the equation may be Laplace transformed simply in the time variable. The initial conditions on the time variable are normally assumed to be zero, and the boundary conditions on the space variable are assumed to be arbitrary. The resulting equations relate the N boundary conditions assumed known to response variables at various spatial locations in the system. The solution of the ordinary linear equation in the space variable for the response w at some spatial location can follow any of several approaches. When the system is arranged as a serial connection of such subsystems it is convenient to relate the subsystem boundary conditions at the interface by means of *transfer matrices*. Transfer matrices are equally applicable to lumped parameter models of system components. For a complete discussion of

transfer matrices and their general use the reader is referred to the book by Pestel and Leckie [10].

A relevant example of a distributed parameter element is the uniform beam modeled by the Bernoulli-Euler beam equation shown below.

$$\partial^4 w / \partial z^4 = (-\mu/EI)(\partial^2 w / \partial t^2)$$

where

- w = the displacement of the neutral axis of the beam from undeformed
- z = the location of a point measured along the neutral axis
- μ = the mass density per unit length
- EI = the bending stiffness

Alternatively the equation can be expressed in state variable form after the time to frequency domain transformation to obtain

$$\frac{d}{dt} \begin{bmatrix} -w \\ \psi \\ M \\ V \end{bmatrix} = \begin{bmatrix} 0 & 1 & 0 & 0 \\ 0 & 0 & 1/EI & 0 \\ 0 & 0 & 0 & 1 \\ \mu\omega^2 & 0 & 0 & 0 \end{bmatrix} \begin{bmatrix} -w \\ \psi \\ M \\ V \end{bmatrix}$$

where

- ψ = the slope of the neutral axis
- M = the bending moment at a beam cross section
- V = the shear at a beam cross section

The variables w (or $-w$), ψ , M , and V are the transfer matrix state variables. The negative of w is used to achieve the symmetry about the cross diagonal. They are generally convenient for specifying boundary conditions as well. The above matrix differential equation can be solved with state variable techniques, assuming an arbitrary boundary condition at $z=0$, for the values of the state variables at $z=L$, where L is the length of the beam. The results are easily transformed to the beam transfer matrix form shown below.

$$\begin{bmatrix} -w \\ \psi \\ M \\ V \end{bmatrix}_L = \begin{bmatrix} C0 & LC1 & aC2 & aLC3 \\ \beta^4 C3/L & C0 & aC1/L & aC2 \\ \beta^4 C2/a & \beta^4 Lc3/a & C0 & LC1 \\ \beta^4 C1/aL & \beta^4 C2/a & \beta^4 C3/L & C0 \end{bmatrix} \begin{bmatrix} -w \\ \psi \\ M \\ V \end{bmatrix}_0$$

where

- $C0 = (\cosh\beta + \cos\beta)/2$
- $C1 = (\sinh\beta + \sin\beta)/2\beta$
- $C2 = (\cosh\beta - \cos\beta)/2\beta^2$
- $C3 = (\sinh\beta - \sin\beta)/2\beta^3$
- $\beta^4 = -s^2 L^4 \mu/EI$
- $a = L^2/EI$
- s = the complex Laplace variable, units 1/time.

The use of the transfer matrix in conventional analysis can be found in [10] or as it can be applied to manipulators in [3] and [2]. It should be mentioned that this implementation makes no approximations to the distributed nature of the Bernoulli-Euler beam model. Linearity of the describing equations is required, however. Furthermore, although the formulation lends itself to several forms of analysis, synthesis

procedures for frequency domain models tend to be less powerful than for time domain models.

3.3 Conversion From Transfer Matrix to State Variable Model. The transfer matrix method is a useful technique for modeling linear mixed lumped-distributed parameter systems. In particular it provides a systematic means for computation of system eigenvalues, mode shapes, and transfer functions which is well suited to computer implementation. However, it is limited to graphical frequency domain techniques in the controller design problem. For the case of multivariable controller design, state variable methods which permit direct computer solution of control parameters are more desirable.

In this section, a procedure for conversion from a transfer matrix model to an approximate state variable model for the purpose of controller design is discussed. It is based on the representation of the system's response with a decoupled truncated modal model. The justifications for a truncated model are the usual ones; i.e., bandlimited sensors and actuators, and inaccuracy of the model at higher frequencies. Furthermore, the iterative nature of the design technique in Section 4 suggests the possibility of a modal model of relatively low order, depending on control objectives. The nature of the approximations involved in modeling a distributed parameter system with non-selfadjoint boundary conditions is less straightforward [9]. Orthogonality of the mode shapes cannot be guaranteed by the usual arguments. The complete issue is one that merits further study. In this paper the accuracy of the approximation is checked by reverting to the transfer matrix model for verification of the proper controlled system behaviour.

3.3.1 A Decoupled Modal Expansion of the Frequency Domain Model. The state variable model used to approximate the transfer matrix model is the Jordan canonical form developed from (1)

$$\begin{aligned} dx/dt &= \Lambda x + Bu \\ y &= Cx \end{aligned} \quad (2)$$

where n states, m inputs, and p outputs are assumed. Since there are no repeated eigenvalues

$$\Lambda = \text{diag}(\lambda_1 \dots \lambda_n) \quad (3)$$

where λ_i is the i th eigenvalue of the system.

Equation (2) is related to the transfer matrix model as follows. Since we are assuming the response $y(z,t)$ can be approximated with a decoupled modal model, it can be written as

$$y(z,t) \approx \sum_{i=1}^n w_i(z)x_i(t)$$

where $w_i(z)$ is the mode shape associated with the i th eigenvalue and $x_i(t)$ is its time dependent amplitude, or modal coordinate. An output $y_j(t)$ is taken as the response measured at a location z_j in the system:

$$y_j(t) = y(z_j, t) = \sum_{i=1}^n w_i(z_j)x_i(t).$$

In vector form:

$$y(t) = Cx(t); c_{ij} = w_j(z_i) \quad (4)$$

Thus the feed through matrix D in (1) is zero. If equation (2) is Laplace transformed and zero initial conditions are assumed, then a matrix transfer function $G_n(s)$ is:

$$G_n(s) = C(sI - \Lambda)^{-1}B \quad (5)$$

This transfer function approximates that exact one ($G_{im}(s)$) computed numerically with the transfer matrix model:

$$\begin{aligned} G_{im}(s) &\approx G_n(s) = C(sI - \Lambda)^{-1}B \\ G(s) &\approx C(sI - \Lambda)^{-1}B \end{aligned} \quad (6)$$

The approximation in the above equation is used to derive an approximate state variable model. Since the system's eigenvalues and mode shapes can be computed with the transfer matrix method, Λ and C are known. Thus equation (6) must be solved for B to complete the approximation.

The remainder of this section describes the computation of Λ , C , and B with the transfer matrix model.

3.3.2 Obtaining the Plant Matrix. As mentioned, the Λ matrix is given by equation (3). The transfer matrix model can be used to compute the exact eigenvalues of the mixed lumped-distributed parameter system. A brief discussion follows. For a detailed formulation see [10]. For a discussion of a computer program to do this computation see [5] and [6].

The system is composed of a serial connection of modeling components. Each component is represented by its transfer matrix, which relates a vector of variables at one end of the component to those at the other end as a function of the Laplace variables. Such a transfer matrix is described in section 3.2. The system is considered as a whole by multiplying its component transfer matrices. This results in a single system transfer matrix $P(s)$ relating the transfer matrix state vector v_1 at one end of the system to v_0 at the opposite end:

$$v_1 = P(s)v_0$$

The application of system boundary conditions constrains half of the variables of v_1 and v_0 to known values, commonly zero. A homogeneous subset of equations can then be identified:

$$0 = P_h(s)v_h. \quad (7)$$

Assuming v_h is nonzero, the above equation requires that

$$\det[P_h(s)] = 0. \quad (8)$$

Values of s for which this equation holds are the eigenvalues of the system. For complicated systems, they are best computed numerically by applying a root finding algorithm to equation 8.

3.3.3. Obtaining the Output Matrix. As shown in section (3.2), the elements of the output matrix C are the system modes evaluated at the output locations:

$$c_{ij} = w_j(z_i)$$

Mode shapes are computed with the transfer matrix method by substituting an eigenvalue λ_i into the transfer matrix relationships for the model elements. Equation (7) gives

$$P_h(s_i)v_h = 0.$$

If $P_h(s_i)$ is of dimension n and of rank q , where q is less than or equal to $n-1$, then the above equation is solved by initializing $n-q$ elements of v_h . The resulting q -dimensional nonhomogenous problem can be solved numerically (e.g., Gauss-Jordan Elimination). In general, for eigenvalues of unit multiplicity, $q = n-1$.

Once v_h is known, the mode shape is computed by multiplying transfer matrices, which allows computation of the output variable anywhere in the system to within an arbitrary scaling constant. The values of the C matrix are obtained by taking the mode shape values at the output location.

3.3.4. Obtaining the Input Matrix. As was shown in equation 6, the modal state variable model is related to the transfer matrix model through the transfer function matrix. Since $G_{im}(s)$, C , and Λ can be computed with the transfer matrix method, the above equation represents one way to compute B , which can be computed so as to minimize the error between the two models for some set of numerical values

of the Laplace variable s . It should be noted that there are other approaches for computation of \mathbf{B} . One is to decompose the spatial distribution associated with the manipulators forcing the system into the system mode shapes, as in [9]. Another would be to view the problem as one of computing the transfer function's residues, perhaps by contour integration. The approach used here is to compute \mathbf{B} numerically so as to give the least squares solution to (6) for specified values of s .

For a given input u_k , the k -th column of $\mathbf{G}(s)$, $\mathbf{g}^k(s)$ is computed from the transfer matrix model for a specific value s_i which is some value other than an eigenvalue. This is related to the k -th column of \mathbf{B} as:

$$\mathbf{g}^k(s_i) = \mathbf{C}(s_i\mathbf{I} - \mathbf{A})^{-1}\mathbf{b}^k.$$

If this is repeated r times, then the following set of equations result:

$$\begin{aligned} \mathbf{g}^k(s_1) &= \mathbf{C}(s_1\mathbf{I} - \mathbf{A})^{-1}\mathbf{b}^k \\ \mathbf{g}^k(s_2) &= \mathbf{C}(s_2\mathbf{I} - \mathbf{A})^{-1}\mathbf{b}^k \\ &\vdots \\ \mathbf{g}^k(s_r) &= \mathbf{C}(s_r\mathbf{I} - \mathbf{A})^{-1}\mathbf{b}^k. \end{aligned}$$

These can be written in matrix form with obvious equivalences as

$$\mathbf{g}^k = \mathbf{X}\mathbf{b}^k. \quad (9)$$

For n states, p outputs, and m inputs, \mathbf{g}^k is of dimension $pr \times 1$, \mathbf{X} is $pr \times n$, and \mathbf{b}^k is $n \times m$.

The least squares solution of (9) (minimizing the Euclidian norm of $\{\mathbf{g}^k - \mathbf{X}\mathbf{b}^k\}$) is obtained by application of a singular value decomposition algorithm [8] [7]. While this should minimize the error between the two models for the values of s chosen, the problem of how to best choose both the values of s and the number of values to be used to obtain the best combination of model accuracy and computational efficiency is unresolved. Preliminary studies seem to indicate that several values chosen in the neighborhood of each eigenvalue in the model give good results for the frequency range relevant to the modal model.

4 State Space Design With Frequency Domain Model Update

In this section the modeling techniques discussed in the previous section will be used to develop a new approach to the design of controllers especially applicable to systems of a distributed parameter nature.

4.1. The Model Update Concept. The state space design of distributed parameter systems using modal models suffers because the decoupling of modes achieved by the modal model is not maintained when the control algorithm is instituted or modified. The feedback control is in effect a modification of the boundary conditions of the distributed parameter components. Many so called "modal" models are not decoupled in the first place. Only the components of these models when originally placed under some simplified, known, constant boundary conditions are decoupled. The result is that the dimension of the state vector must be greater than the actual number of modes of interest to maintain the accuracy of the lower frequency modes.

If the complete distributed model were to be checked after the control parameter selection it would be found that the behaviour of the system was not as specified in the design procedure. By repeating the design procedure with an updated model it might be possible to converge to the true solution even with a low order state vector. Automation of this procedure requires that the model update process be

automated. For linear systems and controllers this can be accomplished using the transfer matrix techniques described in the previous section. The complete procedure is outlined below.

1. Model the system and control via transfer matrix techniques.
2. Convert the transfer matrix model to a low order state variable modal model.
3. Apply an automated design technique to the current state variable model.
4. Update the state variable model to insure decoupling.
5. Compare the specifications of the updated model to those predicted by the automated design technique.
6. If the specification is satisfied with the desired tolerance the process is complete, otherwise return to 2.

4.2. The State Space Design Algorithm. Choice of the state space design to be used in the proposed scheme will depend on the application at hand. The various optimal regulator and servo algorithms represent a good choice for many systems. In the present application, the control of mechanical arms, the desired behaviour is often described in terms of the poles or eigenvalue locations of the controlled system. This is a convenient choice because of the simplicity of solving for the desired gains and because of the simplicity of comparing the updated model to the design specifications.

An algebraic means for selection of feedback gains presented in Takahashi et al. [11] has been programmed and applied to the simple case described below. This simple case has only one control input (one actuator torque) and has the number of measurements equal to the number of modes in the reduced order state equation. When these special cases are not true the simple analysis described below must be generalized.

Define

$$\mathbf{P} = [\mathbf{b}, \mathbf{A}\mathbf{b}, \dots, \mathbf{A}^{n-1}\mathbf{b}]$$

and define \mathbf{p} as the n^{th} column of $(\mathbf{P}^{-1})'$. The vector of feedback coefficients k which yields the scalar control u

$$u = \mathbf{k}'\mathbf{x}$$

is found simply as

$$k = \sum_{i=1}^n (a_{ic} - a_i)(A^i)^j p$$

where

- a_i = the coefficient of s^i in the open loop characteristic equation
- a_{ic} = the coefficient of s^i in the desired closed loop characteristic equation
- $\mathbf{b} = \mathbf{B}$ for the special case where $m = 1$

4.3. A Simple Example. In order to demonstrate the model update approach to control system design a simple example is given in this section. The simple single input multi-output system is described and then the controller for it is designed. The specification of the dominant poles of the system is achieved in three cases termed stiff, flexible, and floppy. The behaviour of the higher modes is examined and the extension to more complex systems is discussed.

4.3.1. The Example System. The system used in the examples of this section is shown in Fig. 4-1. It is a similar configuration to the example of Fig. 2-1 with some relevant differences. It consists of two Bernoulli-Euler beams joined by a rotational joint. The joint actuator is a torque source with no other dynamics modeled. The inboard beam is joined rigidly to the inertial reference frame. Measurements of the joint angle and angular velocity are assumed available for feedback to the control system. The system parameters are

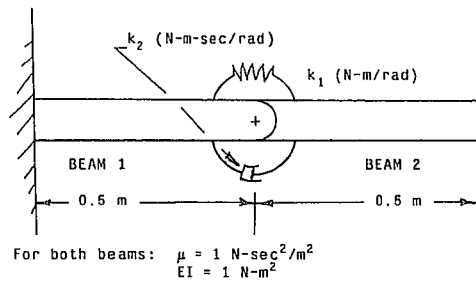


Fig. 4-1 Example arm for control example

Table 4-1 Three cases studied

Case	Behavior	ω/ω_c	Damping ratio
1.	Stiff	0.1	0.707
2.	Flexible	0.386	0.707
3.	Floppy	0.85	0.1

Table 4-2: Convergence of the dominant poles to the specified locations

Iteration number	Dominant Pole Location	
	Real Part	Imaginary Part
Case I, Stiff Behavior		
0	0.0	0.004899
1	-0.349898	0.356381
2	-0.350000	0.349998
3	-0.350000	0.350000
Case II, Flexible Behavior		
0	0.0	0.004898
1	-1.107136	1.819500
2	-1.486605	1.200199
3	-1.377007	1.351059
4	-1.359996	1.360271
5	-1.360000	1.360000
Case III, Floppy Behavior		
0	0.0	0.004898
1	-0.103217	2.323519
2	-0.175495	2.814143
3	-0.250249	2.991617
4	-0.300973	3.005031
5	-0.299966	2.999983
6	-0.300000	3.000000

chosen for ease in visualization and are shown in the figure. The resulting clamped actuator natural frequency ω_c is 3.52 rad/s. Note that an initial rotary spring is provided at the joint. This is equivalent to an initial feedback gain to be adjusted by the design procedure.

The specification of the desired control system performance is in terms of the location of the dominant poles. Three sets of specifications are presented and we will refer to them in terms of the magnitude of the dominant eigenvalues, ω , and the ratio ω/ω_c . The values are given in Table 4-1.

Notice that for case 3 the damping ratio is quite small. With the simple position and velocity feedback control algorithm used, adequate damping for this case is not possible. This is not a fault of the design procedure but of the control algorithm. The design procedure is given a feasible task by keeping the damping ratio to 0.1.

4.3.2. Convergence to the Desired Pole Location. The convergence of the design procedure to the correct specifications (pole locations) is shown in Fig. 4-2 and in Table 4-2.

In the *stiff* case the update procedure is not really required since the state space design procedure alone results in sufficient accuracy on the first iteration. Only a slight improvement is possible and is achieved on the second iteration.

The *flexible* case indicates the true worth of the update procedure. This case exhibits significant interaction of the joint motion and the flexible dynamics of the beams. After

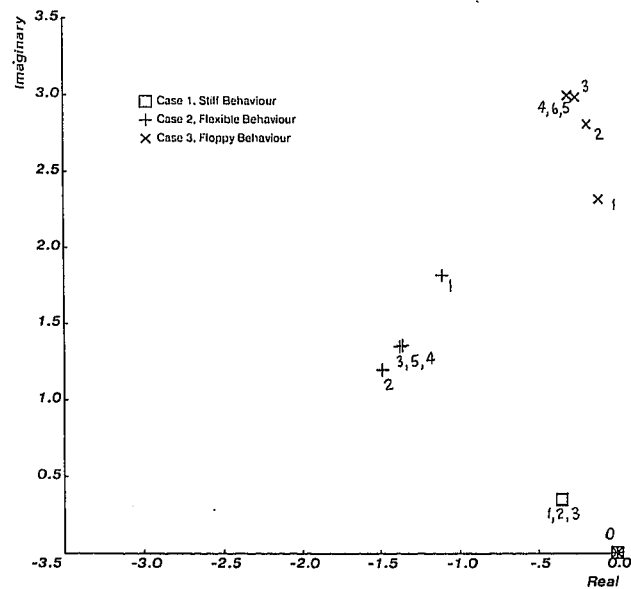


Fig. 4-2 Dominant pole convergence for three design cases

the first iteration the true damping ratio is .52 rather than the desired .707, an error of about 26%. In five iterations the pole location has converged to that specified to within 6 decimal places. Practical convergence is achieved in three iterations.

The *floppy* case requires slightly longer (6 iterations) to converge to the specified pole locations to within 6 decimal places. Practical convergence is achieved in 4 iterations.

4.3.3. Mode Shapes and Higher Modes. Examination of the mode shapes shows some interesting aspects of the control of such flexible systems. The position mode shapes of the uncontrolled system and the three cases of control are shown in Figs. 4-3, 4-4, 4-5, and 4-6 for the first three modes. The frequency of the modes is also given in the figure.

Before control is added one sees in Fig. 4-3 that the first mode corresponds to a largely rigid mode with motion only at the joint. Recall that an initial "spring" is included at the joint causing the first mode to be at a nonzero frequency. After control the rigid case (Fig. 4-4) continues to show no deflection in the beams. The other two cases show significant deflection for the first mode as expected. Furthermore, the rigid case shows minimal shift in the frequency of the second mode while the other two cases show a substantial shift in frequency of the second mode but not the other modes.

The controlled poles and mode shapes generally show a substantial imaginary part indicating vibration in this mode is being damped out by the joint velocity feedback as desired. The exception to this is the third mode. Since this mode shape produces almost no change in angle at the joint, almost no motion of the joint results from this mode in isolation. Thus there is no opportunity for the dissipation of the energy of this mode. This could present a problem for a real arm design with the third mode being of greater concern than the lower frequency second mode. This indicates the importance of checking the higher modes of the system which is easily done with the update procedure that has been implemented.

Higher modes should be checked for another reason. It is possible to specify dominant pole positions that cannot be obtained by the prescribed control algorithm. An example would be poles with a 0.707 damping ratio for the floppy case. The design procedure may succeed in placing a pair other than the dominant pair at that location. This becomes obvious when looking at the mode shapes for the first several modes and their frequency.

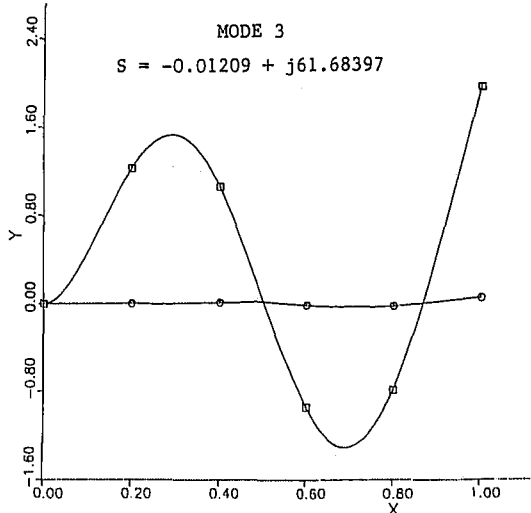
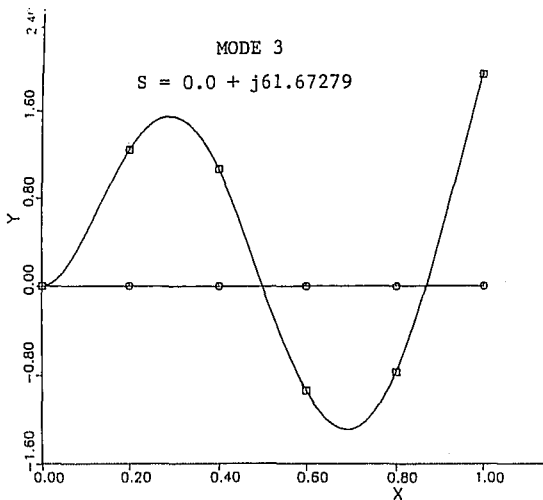
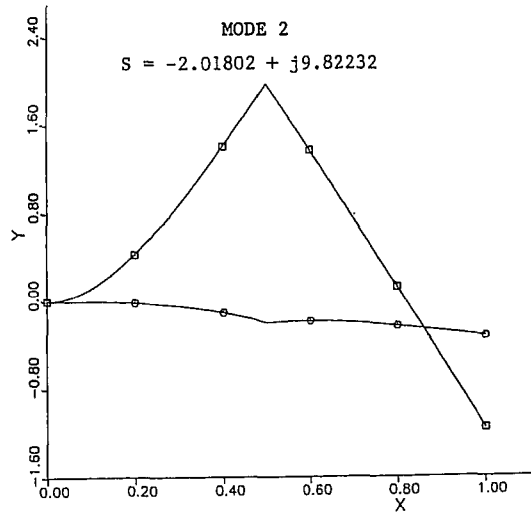
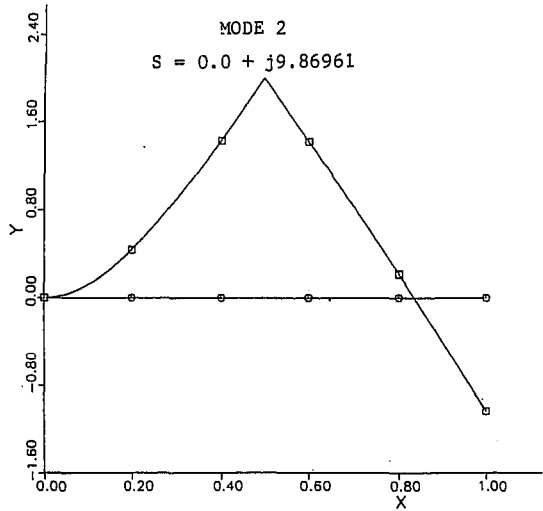
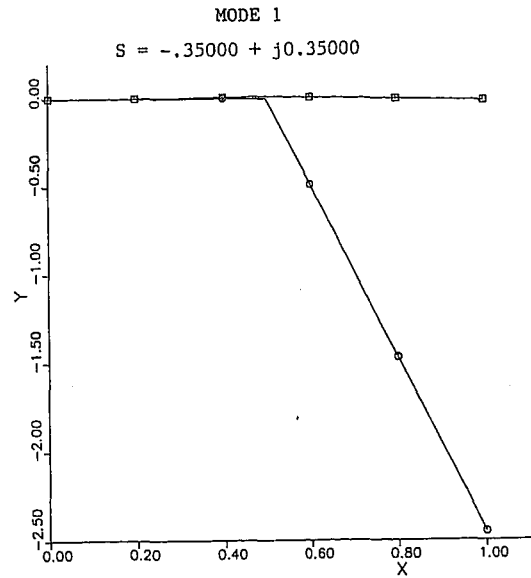
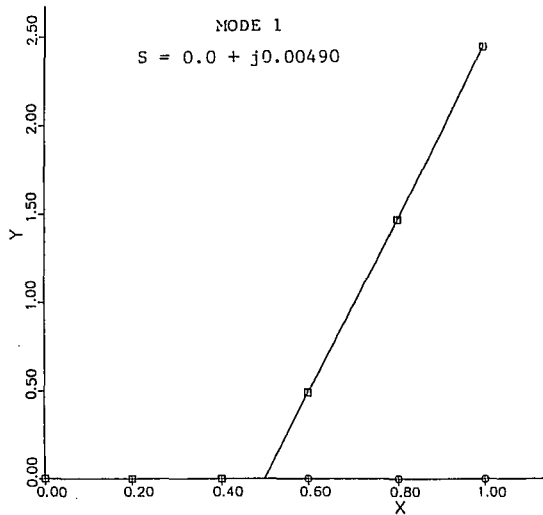


Fig. 4-3 Position modes for the arm without control

Fig. 4-4 Position modes for the stiff case

5 Summary and Conclusions

The practical importance of the control of flexible or compliant arms for high performance but non-exotic applications has been demonstrated, and a new technique for the design of controls for flexible arms has been presented. The reward for this added complexity seems to be greatest for relatively long arms with modest payloads. The size of the reward is dependent on the resolution of a great many details

of the design of a particular arm. The analysis here is only intended to be a preliminary indication of the reward. Before this approach is practical and commonly accepted in the user community a great deal of research and development will be necessary. The advancement of tactile, visual and other means

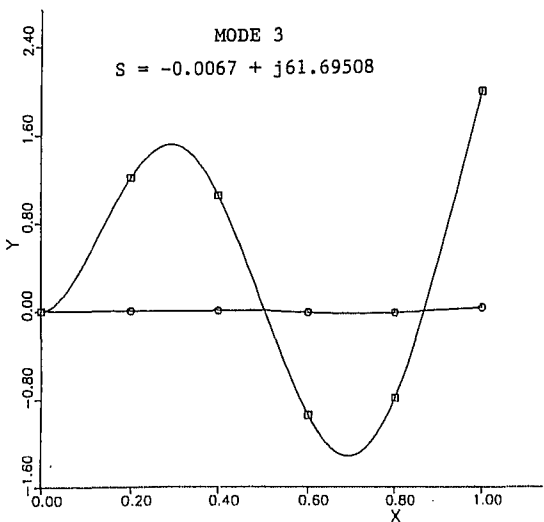
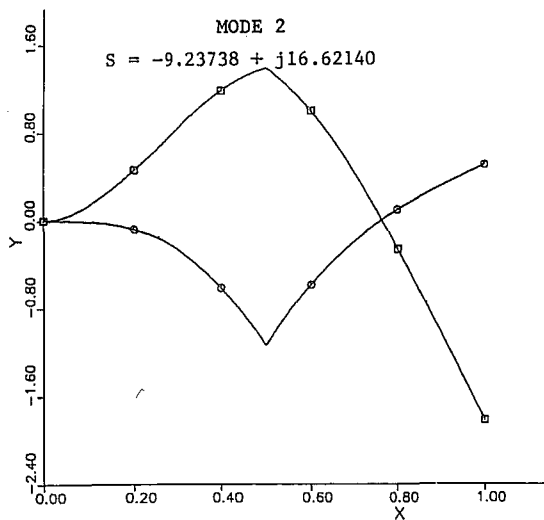
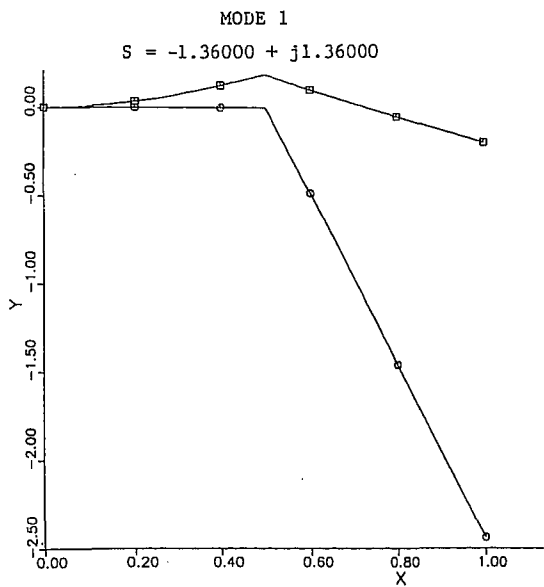


Fig. 4-5 Position modes for the flexible case

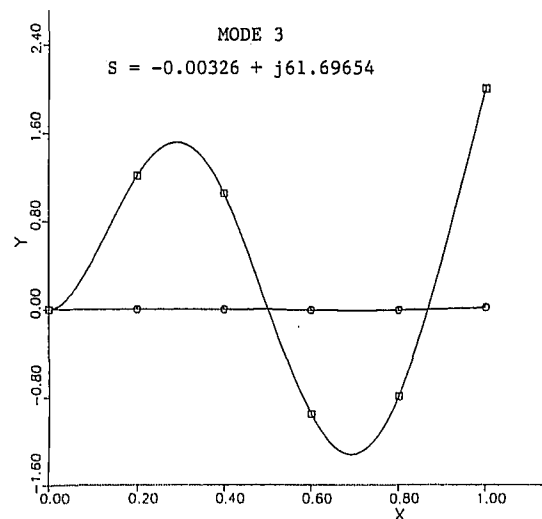
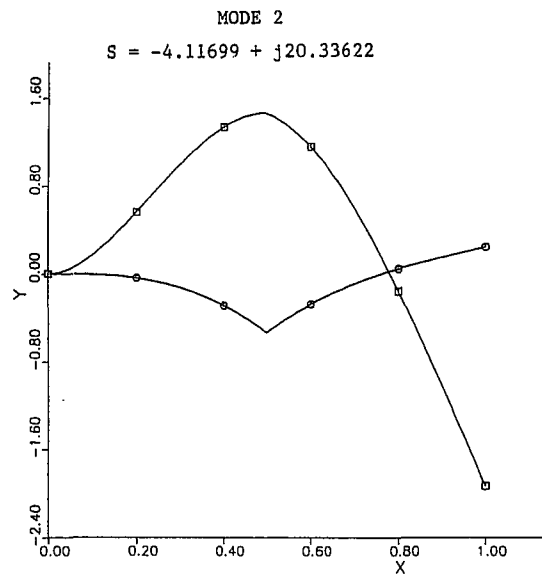
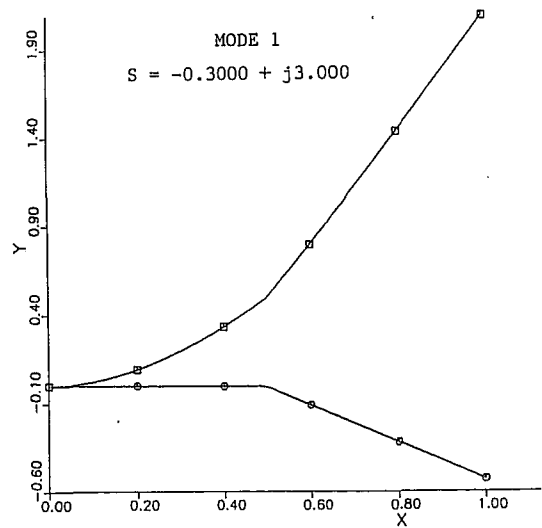


Fig. 4-6 Position modes for the floppy case

of sensing at the endpoint will make this advancement even more beneficial.

The combination of state space and frequency domain techniques through a model update procedure has been shown

effective in determining the feedback gains of a simple distributed parameter, flexible system. The technique seems applicable to control of arms and other distributed parameter systems that can be approximated as linear over a range of

operation. This technique uses a frequency domain, distributed parameter model to update a lower order modal state variable model to maintain decoupling. While transfer matrices were used to implement the frequency domain model here, other implementations, such as with finite element techniques might be more appropriate in other applications. Conventional state variable design techniques are then applied to the low order model. The controller gains are incorporated in the frequency domain model when the next update of state variable model is made. Further consideration should be given to this technique. Variation of some aspects of the approach used here should be tried and some theoretical questions on the assumptions made should be resolved. Specifically, application to more complex multi-input systems and systems with fewer measurements than controlled modes should be considered. Alternative ways of determining the input matrix B are needed. One alternative might be obtaining the zeros from the frequency domain model which could then be used in standard canonical forms of the system equations. A study of the most suitable in terms of overall computational efficiency and accuracy could then be performed. Assumptions about the suitability of the modal approximation for non-conservative distributed parameter systems were justified on a physical basis but should receive more theoretical attention.

Acknowledgments

This work was supported in part by the National Aeronautics and Space Administration and the Charles Stark Draper Laboratory, Inc. with NASA contract NAS9-13809, subcontracts 551 and 586. Portions of the work were performed while the first author was at The Robotics Institute at

Carnegie-Mellon University as Visiting Scientist. The support of the Robotics Institute is also acknowledged.

References

- 1 Balas, Mark J., "Feedback Control of Flexible Systems," *IEEE Transactions on Automatic Control* AC-23, 4 1978, pp. 673-679.
- 2 Beazley, William G., "The Small Motion Dynamics of Bilaterally Coupled Kinematic Chains with Flexible Links," Ph.D. thesis, The University of Texas at Austin, Dept. of Mechanical Engineering, Aug. 1978.
- 3 Book, Wayne J., Modeling, *Design and Control of Flexible Manipulator Arms*, Ph.D. thesis, Massachusetts Institute of Technology, Dept. of Mechanical Engineering, Apr. 1974.
- 4 Book, Wayne J., Maizza-Neto, O., and Whitney, D. E., "Feedback Control of Two Beam, Two Joint Systems with Distributed Flexibility," *ASME JOURNAL OF DYNAMIC SYSTEMS, MEASUREMENT, AND CONTROL*, Vol. 97, No. 4, Dec. 1975.
- 5 Book, Wayne J., Majette, Mark, and Ma, Kong, "The Distributed Systems Analysis Package (DSAP) and Its Application to Modeling Flexible Manipulators, Georgia Institute of Technology, School of Mechanical Engineering, July 1979. Subcontract No. 551 to Charles Stark Draper Laboratory, Inc., NASA contract no. NA9-13809.
- 6 Book, Wayne J., Majette, Mark, and Ma, Kong, "Frequency Domain Analysis of the Space Shuttle Manipulator Arm and Its Payloads; Vol. I—Analysis and Conclusions; Vol. II—Computer Program Description and Listings," Georgia Institute of Technology, School of Mechanical Engineering, Feb., 1981. Subcontract no. 586 to Charles Stark Draper Laboratory, Inc., NASA contract no. NAS9-13809.
- 7 Lawson, Charles L., and Hanson, R. J., *Solving Least Squares Problems*, Prentice-Hall, Inc., 1974.
- 8 Dongarru, J. J., Moler, C. B., Bunch, J. R., and Stewart, G. W., *LINPACK User's Guide*, SIAM, 1979.
- 9 Murray-Lasso, M. A., *The Model Analysis and Synthesis of Linear Distributed Control Systems*, Ph.D. thesis, Massachusetts Institute of Technology, Nov. 1966.
- 10 Pestel, E. C., and Leckie, F. A., *Matrix Methods in Elastomechanics*, McGraw-Hill, 1963.
- 11 Takahashi, Y., Rabins, M. J., and Auslander, D. M., *Control*, Addison-Wesley, 1972.